

Using Ice Crystal Analogues to Validate Cloud Ice Parameter Retrievals from the CPI Ice Spectrometer Data

Z. Ulanowski¹, P. Connolly², M. Flynn², M. Gallagher², A.J.M. Clarke¹ and E. Hesse¹

¹Science & Technology Research Institute, University of Hertfordshire, Hatfield, Herts AL10 9AB, United Kingdom.

²Physics Department, UMIST, Manchester M60 1QD, United Kingdom.

E-mail: z.ulanowski@herts.ac.uk

P2.8:29
(1175)

Problem

- *In situ* probes like the Cloud Particle Imager (CPI) have never been calibrated against realistic particles of known dimensions.
- Sizing accuracy and the influence of defocus on size and concentration estimates are not known.
- The ability to determine crystal shape is uncertain, especially for smaller sizes.

Solution: ice crystal analogues

- Stable at room temperature.
- Correct refractive index: 1.31 at visible wavelengths.
- Hexagonal symmetry.
- Common shapes are available: columns, plates, rosettes, aggregates with sizes <1 μm to >500 μm, including rough crystals

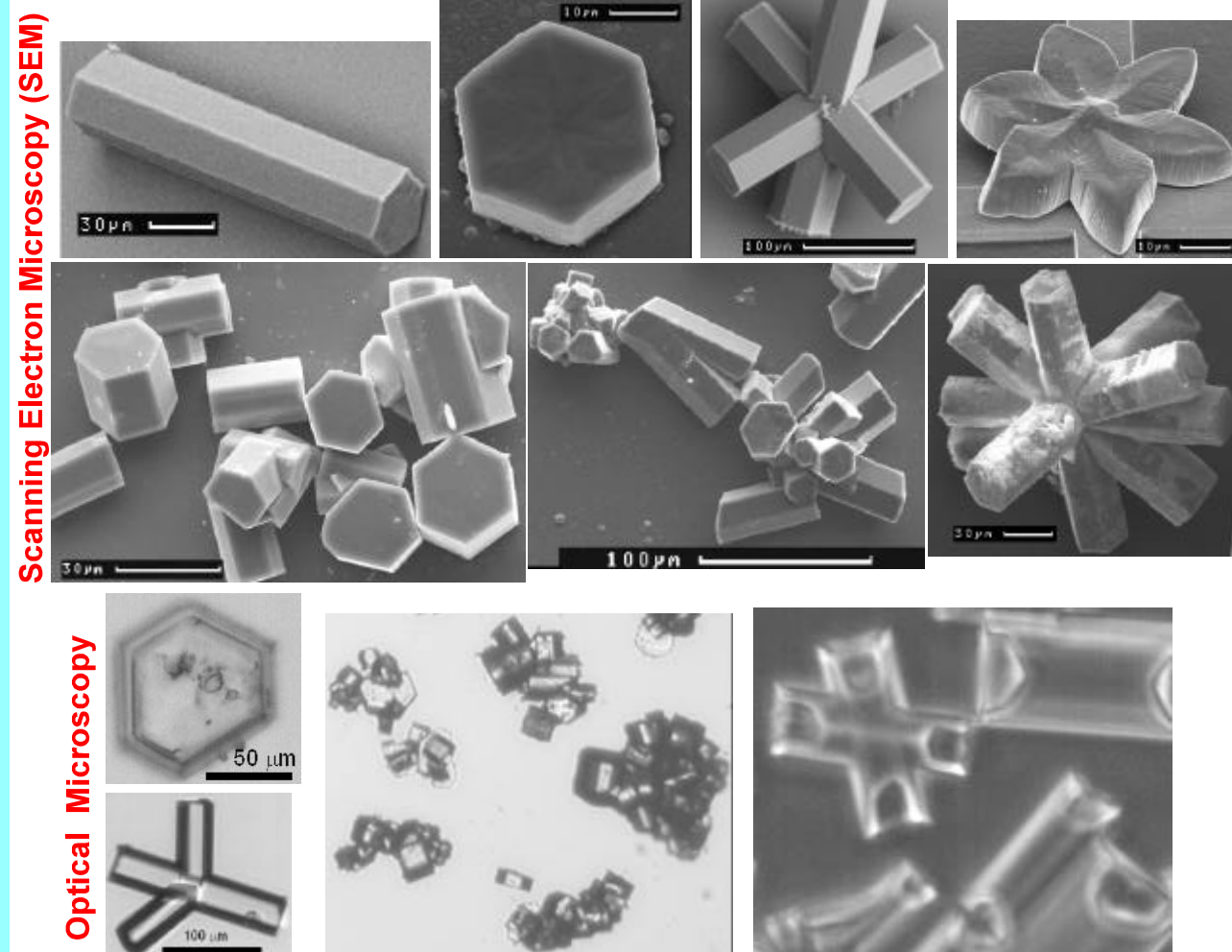


Fig. 1. Example ice-analogue crystals.

Method

- Select single ice-analogue crystals.
- Get optical and SEM images to determine precise shape/size.
- Put crystals on glass slides.
- Insert into CPI and collect images at different positions.
- Compare max. size, area, volume, and r_{equ} from SEM and CPI.

MATERIALS AND PROCEDURES

The ice analogues were crystalline particles of sodium fluorosilicate Na_2SiF_6 grown from solution on glass substrates (Ulanowski *et al.* 2003). Single crystals were selected using a micromanipulator and transferred onto microscope coverslips. The shape and dimensions of the crystals were then determined using low-vacuum scanning electron and optical microscopy - Fig. 1. Further examples can be found at <http://strc.herts.ac.uk/ls/lse.html>. For complex crystals, the shape was determined by constructing a 3-dimensional geometric model on the basis of images taken at different crystal orientations.

The crystal-containing coverslips were attached to a 3-axis translation stage and inserted into the imaging path of the CPI, with their surface perpendicular to the optical axis. The stage permitted varying the distance of the coverslips from the object plane of the imaging system. The CPI was triggered continuously to allow measurements on stationary samples. Since position-sensitive triggering was not used, image acceptance for further analysis was based on the sharpness of the crystal image - the "focus" measure given by the CPI.

The single scattering properties of ice crystals were calculated using geometric optics enhanced by the inclusion of diffraction on facets. The model is a 3-dimensional extension of a method previously applied to long hexagonal columns (Hesse *et al.* 2003).

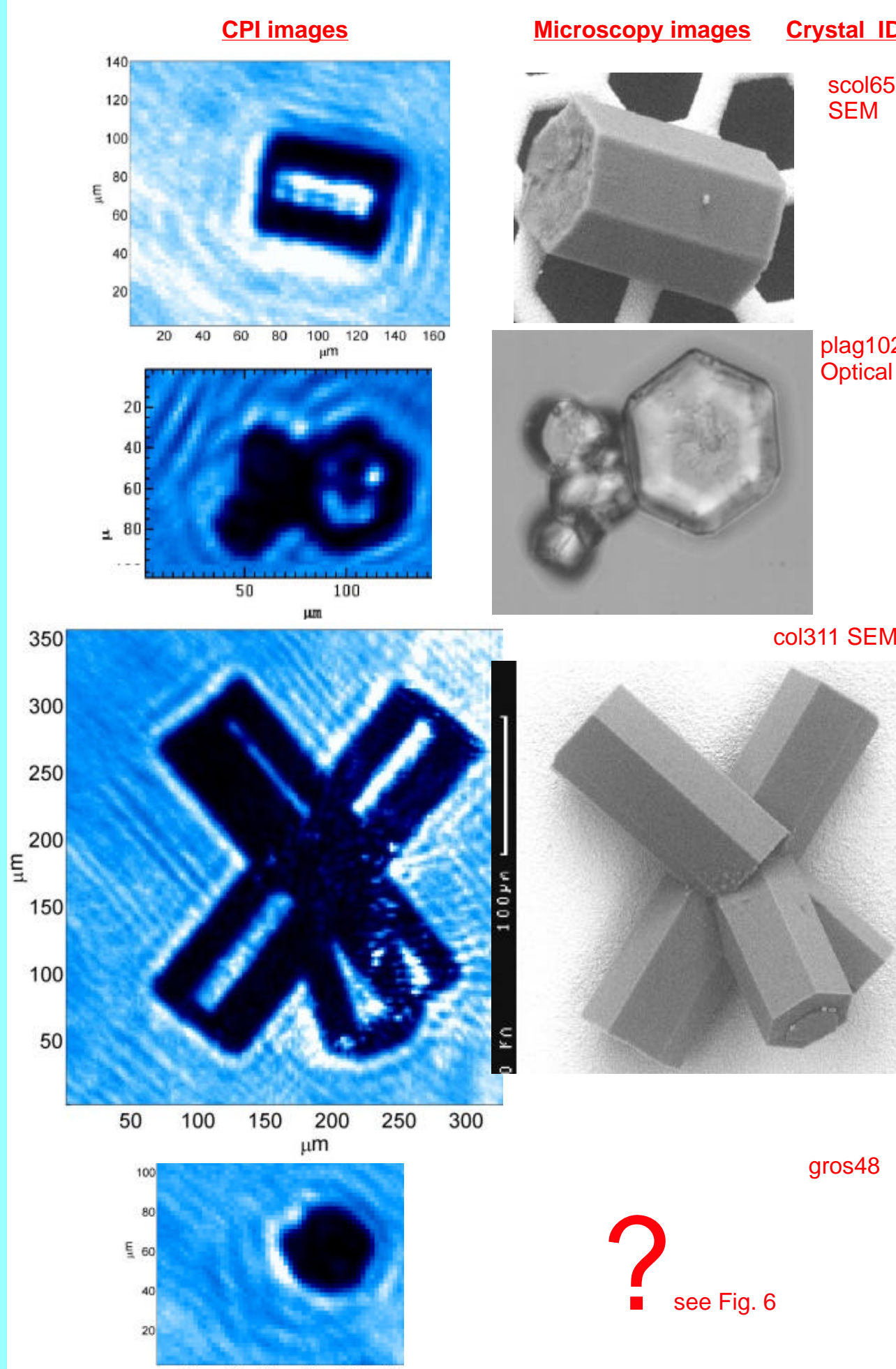


Fig. 2. Comparison of CPI images (left column) and electron or optical microscopy images (right column) of example ice-analogue crystals used in this work. Note that the magnifications are not all identical.

Sizing accuracy

- How accurate is ice crystal sizing using the CPI?
- What is the effect of defocus on size, projected area and volume?

Table 1. Examples of ice crystal analogues used in this work. Shown are the actual (determined from microscopy) maximum dimension D , width W (normal to D), projected area A and volume V , and ratios of measured to actual parameters for two focus criteria: good focus (>50, upper value) and medium to good focus (>20, lower value, in red). Mean standard deviation is given; ND = not determined; for the columns the actual length and diameter are given in brackets. The relations for obtaining V_{mes} were from: H04 - Heymsfield *et al.* (2004), M90 - Mitchell *et al.* (1990), M96 - Mitchell (1996), BF95 - Brown and Francis (1995), COL/SPH - solid circular cylinder for columns or solid sphere for complex crystals.

shape	name	D_{act} (μm)	W (μm)	A_{act} (μm ²)	V_{act} (μm ³)	$D_{\text{mes}}/D_{\text{act}}$ (-)	$A_{\text{mes}}/A_{\text{act}}$ (-)	$V_{\text{mes}}/V_{\text{act}}$ (-)	H04	M90	M96	COL/SPH
column	col50	51.7 (50.2)	24.1 (12.4)	623	5000	1.15 ± 0.09	1.98 ± 0.62	15 ± 3.8	7.7 ± 1.6	8.6 ± 1.8	ND	5.4 ± 3.0
column	scol65	85.1 (67.1)	82.5 (52.3)	3510	127000	0.98 ± 0.07	0.37 ± 0.23	0.95 ± 0.25	0.43 ± 0.10	0.59 ± 0.11	ND	0.36 ± 0.52
column	col166	173 (168)	83 (42.9)	7210	201000	1.03 ± 0.04	0.92 ± 0.31	7.2 ± 0.5	3.1 ± 0.3	2.8 ± 0.2	ND	1.9 ± 0.5
plate	pla102	108	89	7240	200000	1.01 ± 0.08	0.92 ± 0.39	3.0 ± 0.7	0.98 ± 0.19	ND	0.65 ± 0.12	3.0 ± 0.7
compact	gros48	46.8	41.7	1307	22025	1.04 ± 0.08	1.07 ± 0.35	3.2 ± 0.6	1.07 ± 0.19	ND	0.70 ± 0.12	3.4 ± 0.8
4-arm	ros172	178	135	12700	540000	1.19 ± 0.17	1.64 ± 0.53	3.3 ± 1.6	1.56 ± 0.64	ND	1.27 ± 0.44	4.2 ± 2.0
rosette	ros172	178	135	12700	540000	0.98 ± 0.04	0.94 ± 0.29	2.7 ± 0.2	1.19 ± 0.12	ND	0.66 ± 0.06	4.9 ± 0.8
rosette	ros172	178	135	12700	540000	0.99 ± 0.04	0.99 ± 0.32	2.8 ± 0.2	1.25 ± 0.14	ND	0.69 ± 0.07	5.3 ± 0.8
plate	plag102	104	75.2	4650	114000	0.98 ± 0.05	1.02 ± 0.29	4.3 ± 1.0	1.40 ± 0.21	2.2 ± 0.25	ND	4.5 ± 3.0
aggr.	aggr.					1.02 ± 0.07	1.13 ± 0.14	5.0 ± 0.6	1.56 ± 0.27	2.4 ± 0.32	ND	5.1 ± 1.0

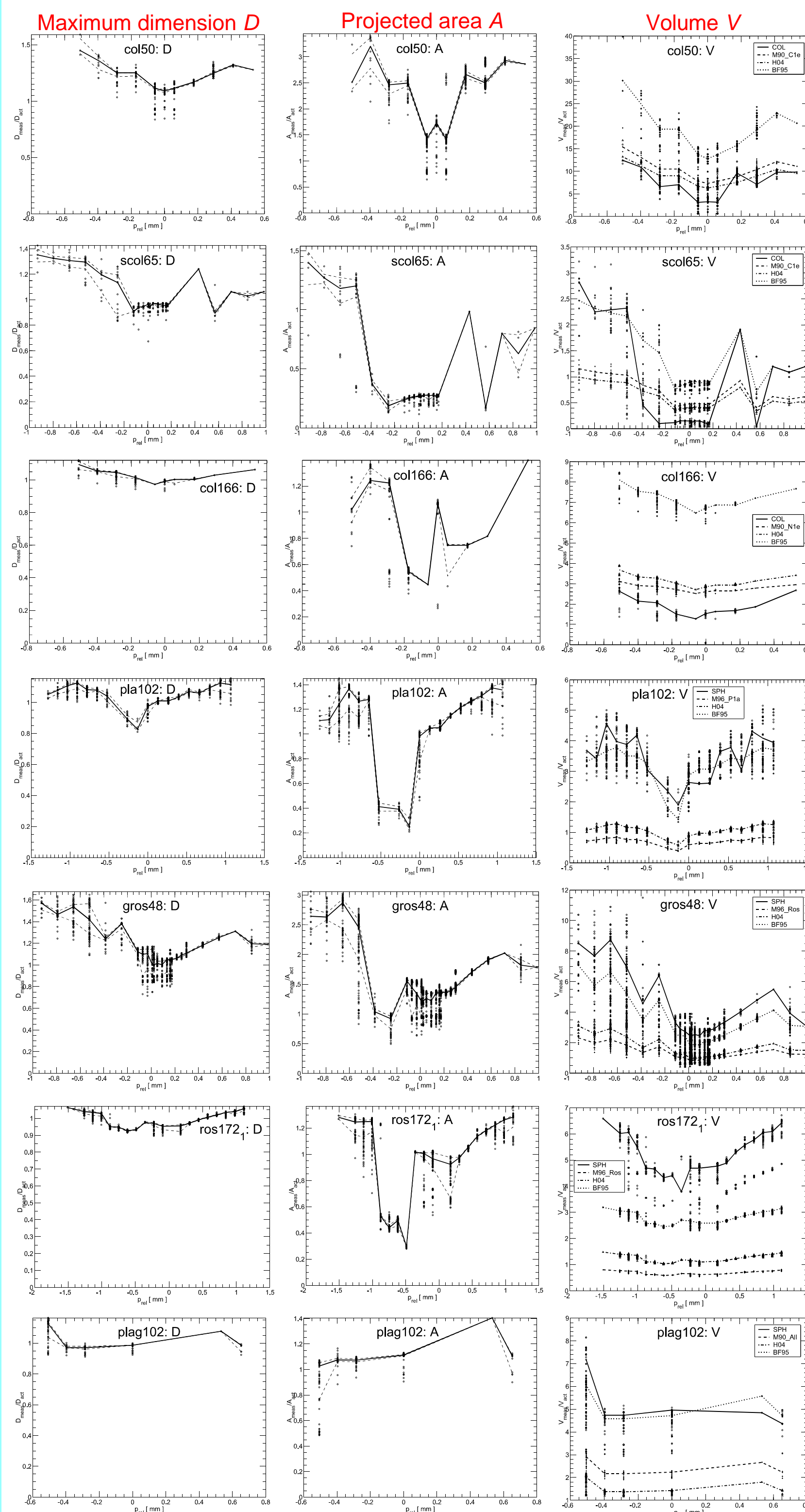


Fig. 3. Ratio of measured to actual (determined from microscopy) maximum dimension D , projected area A , and volume V for the ice-analogue crystals from Table 1, shown as a function of the distance from the CPI object plane. Quartiles (broken line) and medians (solid line) are shown for D and A , and medians for V . Volume relations are as in Table 1: BF95 (+, dotted line), H04 (Δ, dot-dash), M95 or M96 (•, broken line), COL/SPH (○, cont. line).

The CPI-derived crystal size D depends on the position of the particle with respect to the object plane of the imaging system (defocus). The size in general increases with the defocus, leading to maximum overestimates for smaller crystals of up to 60%, and for crystals >100 μm of up to 10%. Typical mean overestimates are near 20% for the smaller crystals but become much lower for the larger ones. Particles "in focus" are typically sized within a few percent of the actual value - see Table 1.

While the accuracy of volume retrievals follows a general trend similar to that of D , it is strongly affected by the choice of the size to volume relationship, as Table 1 and Fig. 3 show. For this reason we included a simple approximation for column volume, assuming a solid circular cylinder: $V = \pi D(W/2)^2$. It can be expected to overestimate the volume, especially for columns with aspect ratio near one, as both D and W are larger than their column length and diameter, respectively. However, in most cases it gives better results than the other, more complex relations. In contrast, assuming spherical shape for volume calculations of complex crystals gives poor outcome.

The sampling volume within which crystals are counted increases with crystal size. This situation is relevant to cloud observations where crystal number density is so high that several crystals can be present in the CPI. Such conditions make position-sensitive discrimination ineffective. Preliminary estimates indicate that the sampling volume varies approximately as D^3 for crystals <100 μm in size, and becomes nearly constant above that value. Thus small crystal number concentration will be significantly underestimated. We can also expect that under high concentration conditions a positive size bias would be introduced (because the measured size increases with defocus).

Crystal shape

- How well is crystal shape determined, especially for small crystals?
- What are the consequences in terms of scattering properties?

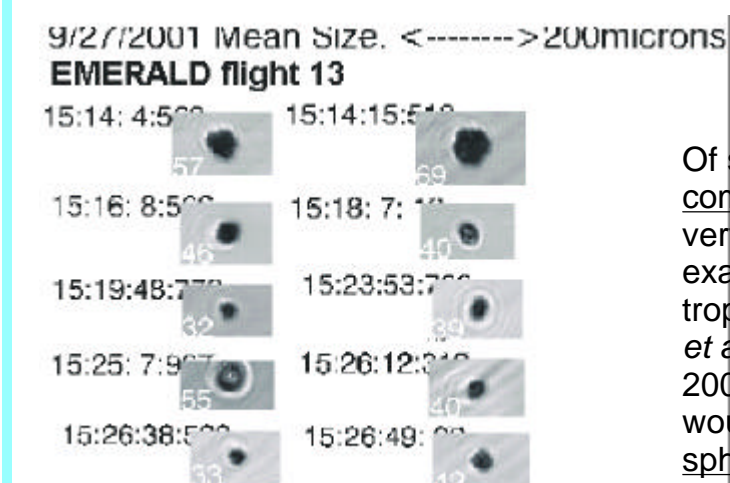


Fig. 4. Typical selection of CPI images of particles classified as "spheroids", sampled during the EMERALD campaign in mid-latitude frontal cirrus.

Of special importance is the case of small, compact crystals. These particles may be very abundant under some conditions, for example in upper cirrus layers or in thin tropical cirrus (Gayet *et al.* 2003, Garrett *et al.* 2003, Hirst *et al.* 2001, Peter *et al.* 2003, Yang *et al.* 2003). Such crystals would normally be classified as spheres or spheroids on the basis of CPI (or other probe) images - see Fig. 4.

Small, compact crystals are represented here by the "germ rosettes" *gros48* and *gros56*. As Figs. 5 and 6 reveal, ice analogue crystals also produce quasi-circular CPI images, even if they are strongly non-spherical like the crystal *gros48*. Therefore we must allow the possibility that the small crystal crystals may be faceted, although their precise identity will remain unclear until better *in situ* probes are deployed. One consequence of assuming spherical shape is overestimation of crystal mass, and hence the Ice Water Content, as the true effective density will be lower than for a sphere (which has effective density of bulk ice) - see Table 1. Note that such error will occur even under good focus conditions: for *gros48* the volume overestimate purely due to assuming spherical shape is by a factor of about 2.4. At poor focus, the mass (- D) was in our tests further overestimated due to sizing errors by an additional factor of about 1.7 on average - see Fig. 3.

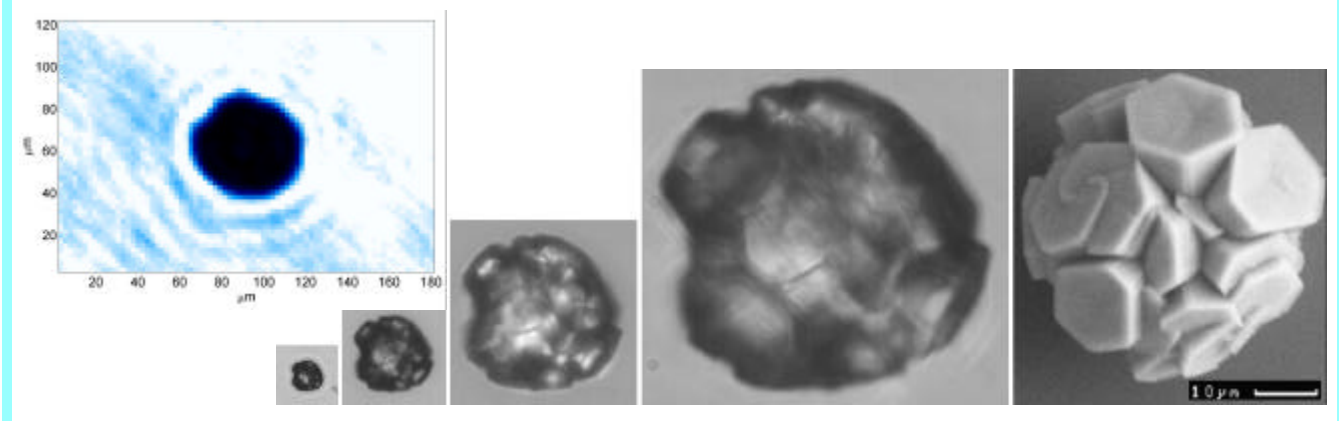


Fig. 5. Ice-analogue rosette *gros56* (maximum dimension 55.3 μm) imaged by the CPI (top left), optical microscope at increasing resolution (centre), and SEM (right).

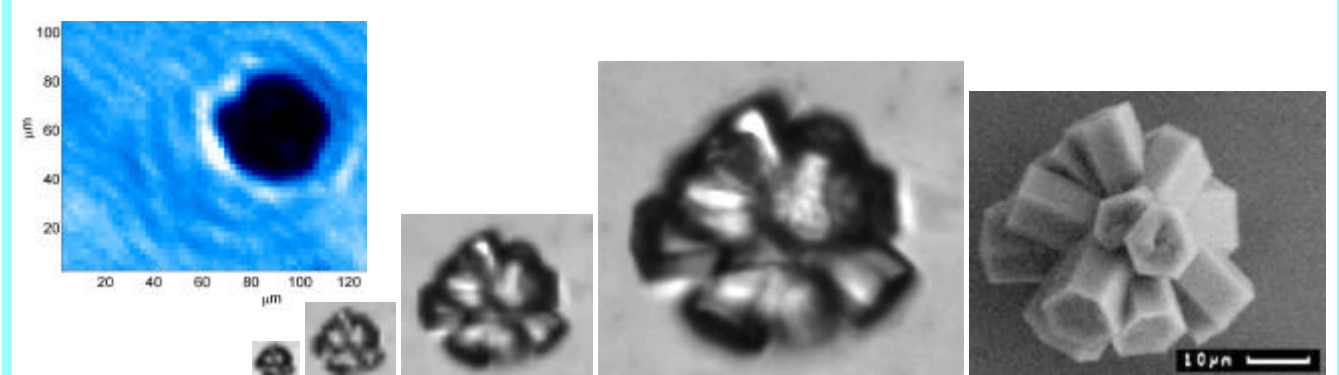


Fig. 6. As Fig. 5, but for the ice-analogue rosette *gros48* (maximum dimension 46.8 μm).

Lack of discrimination between spherical particles and faceted crystals leads also to incorrect inferences concerning single scattering properties. For example, an ice sphere equal in size to the compact rosette *gros48* shown in Fig. 6, has the asymmetry parameter $g=0.881$ at visible wavelengths. In contrast, calculations using the diffraction on facets model (Hesse *et al.* 2003) show that a 20-facet droxtal (Yang *et al.* 2003) of the same size has $g=0.805$ and a compact 8-arm rosette $g=0.776$ - see Fig. 7. Such reduction in g can significantly lower the value of shortwave cloud forcing. For illustration purposes, geometric optics calculations predict that replacing spheres of similar size with polycrystals can reduce net (shortwave and longwave) cloud forcing by nearly 30 W/m^2 (Zhang *et al.* 1999).

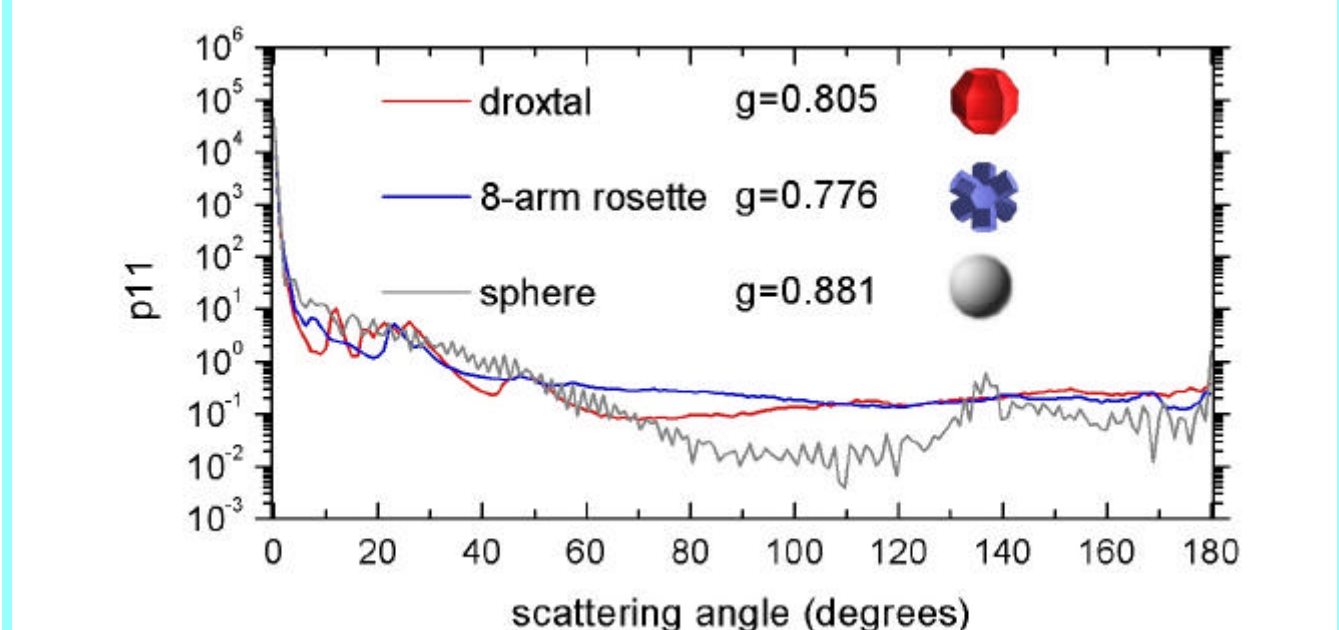


Fig. 7. Phase functions for a sphere, droxtal and 8-arm compact rosette, representing the crystal *gros48*; also shown are the values of the asymmetry parameter g (calculations using Mie theory for the sphere and geometric optics with diffraction on facets for the crystals (Hesse *et al.* 2003)).

Summary

- Typical average size errors are a few % under good focus conditions
- Under poor focus size is significantly overestimated
- Number concentration drops sharply with decreasing size below 100 μm
- Size may be additionally overestimated at high concentrations
- Faceted crystals as large as 50 μm can be misclassified as spheroids
- This can lead to significantly overestimated asymmetry parameter

References

- Brown, P.R.A., and P.N. Francis, 1995: Improved measurements of the ice water content in cirrus using a total-water probe. *J. Atmos. Sci.*, 52, 410-414.
- Garrett T. J., H. Gerber, D. G. Baumgardner, D. G. C. H. Twohy, and E. M. Weinstock, 2003: Small, highly reflective ice crystals in low-latitude cirrus. *Geophys. Res. Lett.*, 30, 2132.
- Gayet, J.-F. *et al.*, 2002: Quantitative measurement of microphysical and optical properties of cirrus clouds. *Geophys. Res. Lett.*, 29, 2230.
- Ghan, S. J., L. R. Leung, and Q. Hu, 1997: Application of cloud microphysics to NCAR community climate model. *J. Geophys. Res.*, 102, 16507-16527.
- Gulterpe, I., G.A. Isaac, A. Korolev, S. Cober, and J.W. Strapp, 1998: Effects of ice crystal shape on the radiative characteristics of low level ice clouds. *Conf. on Cloud Physics*, AMS, Everett, 372-375.
- Hesse, E., and Z. Ulanowski, 2003: Scattering from long prisms using ray tracing combined with diffraction on facets. *J. Quantit. Spectr. Rad. Transf.*, 79-80, 721-732.
- Heymsfield, A. J., C. Schmitt, A. Bansemmer, D. Baumgardner, E.M. Weinstock, J.T. Smith, and D. Sayers, 2004: Effective ice particle densities for cold anvil cirrus. *Geophys. Res. Lett.*, 31, L02101.
- Hirst, E., P.H. Kaye, R.S. Greenaway, P. Field, *et al.*, 2001: Discrimination of micrometre-sized ice and super-cooled droplets in mixed-phase cloud. *Atm. Env.*, 35, 33-47.
- Meyers M.P., P.J. DeMott, and W.R. Cotton, 1992: New primary ice-nucleation parametrizations in an explicit cloud model. *J. Appl. Meteor.*, 31, 708-721.
- Mitchell, D.L., R. Zhang, and R.L. Pitter, 1990: Mass-dimensional relationships for ice particles and the influence of riming on snowfall rates. *J. Atmos. Sci.*, 29, 153-163.
- Mitchell, D.L., 1996: Use of mass- and area-dimensional power laws for determining precipitation particle terminal velocities. *J. Atmos. Sci.*, 53, 1710-1723.
- Peter, T. *et al.* 2003: Ultrathin Tropical Tropopause Clouds (UTTCs): I. Cloud morphology and occurrence. *Atmos. Chem. Phys.*, 3, 1083-1091.
- Ulanowski, Z., E. Hesse, P.H. Kaye, A.J. Baran, and R. Chandrasekhar, 2003: Scattering of light from atmospheric ice analogues. *J. Quantit. Spectr. Rad. Transf.*, 79-80, 1091-1102.
- Yang P., B.A. Baum, A.J. Heymsfield, Y.Hu, H. Huang, S. Tsay, and S. Ackerman, 2003: Single-scattering properties of droxtals. *J. Quantit. Spectr. Rad. Transf.*, 79-80, 1159-1169.
- Zhang, Y., A. Macke, and F. Albers, 1999: Effect of crystal size spectrum and crystal shape on stratiform cirrus radiative forcing. *Atmos. Res.*, 52, 5975.

Website: <http://strc.herts.ac.uk/ls/lse.html>

This research was supported by a NERC grant NER/T/S/2001/00203. We are indebted to Bill Liley for the electron microscopy images.